

Plasma Instabilities in the Plume of a Hollow Cathode

Marcel P. Georjin *, Benjamin A. Jorns,[†] and Alec D. Gallimore[‡]
University of Michigan, Ann Arbor, MI, 48109

Plasma instabilities are spatially characterized in the plume of a 20 A LaB₆ hollow cathode using ion saturation probes. The wave measurements are analyzed using a continuous wavelet transform to decompose the signal into three types of oscillations: 50 kHz, 0.1-0.5 MHz, and 0.8-1.2 MHz. Measurements of the wave amplitude of the 50 kHz oscillation with position show that this instability is localized in the plasma plume and is interpreted as the source for the other instabilities in the plasma. The 0.1-0.5 MHz waves are shown to be dominant near the cathode and are interpreted using ion-acoustic soliton theory. The analytical description of a soliton is in good qualitative agreement the measurement; however, estimates of the width are 1 to 2 orders of magnitude smaller than the observations. Lastly, the waves from 0.8-1.2 MHz are shown to be qualitatively well described by a Gaussian wave packet, though the velocity measured from the dispersion of these waves is too large to be an ion-acoustic wave packet. Together, these measurements support the notion that a localized instability in the cathode plume gives rise to propagating instabilities composed of the natural modes of the plasma including solitons and wave packets.

Nomenclature

I	=	current [A]
\dot{m}	=	mass flow rate [sccm]
α	=	empirical constant [A/sccm]
T_e	=	electron temperature [eV]
V	=	Langmuir probe bias voltage [V]
V_P	=	plasma potential [V]
I	=	probe current [A]
I_{sat}	=	ion saturation current [A]
m_i	=	ion mass [kg]
m_e	=	electron mass [kg]
A_p	=	probe area [m ²]
n_i	=	ion density [1/m ³]
δn	=	plasma density fluctuation [1/m ³]
n_0	=	steady state plasma density [1/m ³]
τ	=	time [s]
t	=	dummy variable of integration [s]
v_{ph}	=	phase velocity [m/s]
v_g	=	group velocity [m/s]
v_e	=	electron thermal speed [m/s]
ω	=	plasma wave frequency [rad/s]
k	=	plasma wavevector [rad/m]
$\chi(\omega, \tau)$	=	continuous wavelet transform amplitude [arb.]
$(\psi)(\omega(t - \tau))$	=	mother wavelet
$w(t)$	=	envelope function

*Ph.D. Candidate, Applied Physics Program, Student Member

[†]Assistant Professor, Department of Aerospace Engineering, and AIAA Senior Member.

[‡]Dean of Engineering, College of Engineering, and AIAA Fellow.

I. Introduction

THE hollow cathode is a device that is commonly used as an electron source for several types of plasma thrusters. The plume of these devices is subject to a variety of plasma instabilities that evidence suggests play a fundamental role in how they operate. These instabilities are believed to dominate the electron and ion dynamics and, in some measure, to enhance the erosion of the cathode keeper. Indeed, for the latter process, the erosion stemming from these instabilities may ultimately be a failure mechanism of Hall and ion type thrusters.¹ This erosion is typically associated with large-scale oscillations in plasma potential that onset in the so-called plume mode.² By including these oscillations empirically into numerical models, it is possible to recover measured erosion rates.³ Hollow cathodes for electric propulsion have been in development for decades and these studies have identified empirical techniques for avoiding the plume mode - namely increasing the flow rate through the cathode. Although we have been successful in mitigating this erosion, this solution has risks and drawbacks. First, because the neutral particle environment changes in space, there is the possibility that this mitigation technique may not work and the plume mode could onset. Second, since we do not have a predictive model for plume mode, it is very challenging to predictively design and assess the life of a cathode. In fact, only one numerical model has resolved an instability that resembles to the plume mode oscillation.^{4,5}

Given the importance of understanding plume mode for cathode life, there have been a number of analytical and experimental studies dedicated to understanding the physics that drives the erosion. For example, the first series of measurements of the instabilities associated with plume mode indicated that they onset at high current or low propellant flow rate.^{2,6,7} Historically, this onset criterion is commonly interpreted as an indication that the plume mode is the result of an ionization type instability. It has been theorized to follow a predator-prey model where the ionization rate rises at sufficiently high current (or low flow rate) leading to a depleted neutral population. This ultimately results in an oscillation in the electron and neutral densities.^{8,9} Although this interpretation may make intuitive sense, the theory does not predict growth and basic fluid models of cathodes do not recover the instability. In fact, there are several interpretations in the literature claiming to describe this oscillation, but none of these have derived a clear onset criterion or identified a source of energy for growth.^{5,10,11} In an effort to improve upon these initial experimental and analytical studies, the plume mode has been characterized experimentally and shown to have complicated spatial structure. Measurements by Goebel et.al. have found that large plasma potential fluctuations at 80 kHz exist in the plume region of the cathode, but are absent in the insert region.⁹ This result suggests that instead of a quasi-zero dimensional predator-prey type mode, the formation of the oscillations may be more nuanced. Following this hypothesis, Georgin et.al. have shown using high-speed imaging and electrostatic probing that structures appear to propagate away from a localized point in the cathode plume region both towards the anode and cathode.^{11,12} Their work offers the interpretation that these propagating modes are possibly ion acoustic solitons and wave packets. This evidence supports the notion that the plume mode oscillation is composed of the natural frequency responses of the plasma to a large scale perturbation. This novel interpretation, while not identifying the source of the point perturbations, has yielded new insight into what the constituent parts of the plume mode oscillations actually are. Furthermore, it is directing our studies to a specific region in the plume as the region of interest for identifying the driving mechanism.

Although this more detailed and nuanced physical picture for this instability is beginning to form from previous work, there remain several questions regarding the nature of the instabilities. Indeed the mechanism that actually leads to the initial perturbation remains unknown. There are several detailed questions about this physical interpretation that remain outstanding. For example, what is the actual nature of the propagating structures away from the perturbation? Are they actually resident modes? Can they give us clues to the origin of the instabilities? Given the conflicting interpretations in the literature and the leading questions about the nature and evolution of the instability, there is a need for more precise experimental measurements of the propagating modes to develop a clearer physical interpretation.

This paper is organized as follows. First, we provide a brief background of the relevant physics. Then we describe the experimental configuration used to probe this instability and the analysis used to understand the constituent modes. We then present the analysis of the experimental results. Finally, we draw some conclusions about the nature of the instabilities.

II. Background

The physical picture guiding our investigation of the plume mode instability is illustrated in Fig. 1, where the plasma plume is quasi-periodically perturbed. This perturbation can be thought of being composed of the natural modes that are believed to propagate in the plasma. Evidence suggests that the response to the perturbation is comprised of solitons and wave packets that propagate away from the source. Below, we will provide the necessary background information for solitons and wave packets to interpret our experimental results.

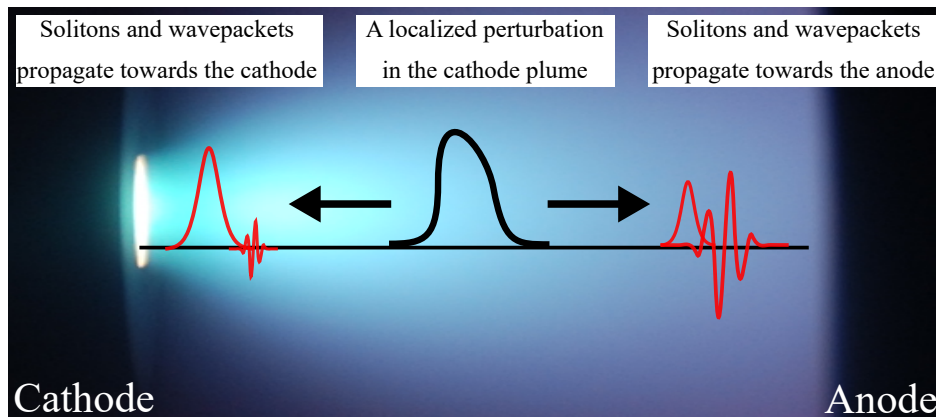


Fig. 1 Illustration of the plume mode instability. A large perturbation is generated in the plasma, which is composed of the modes that can be sustained by the plasma. For the cathode, these modes appear to be solitons and wave packets.

A. Solitons

Solitons in a plasma are a weakly non-linear acoustic wave where the non-linearity of convection is balanced by wave dispersion resulting in a coherent snoidal structure in the plasma.¹³⁻¹⁵ The density fluctuation is

$$\tilde{n} = \delta n \operatorname{sech}^2 \left(\frac{z - ut}{D} \right), \quad (1)$$

where, δn is the soliton amplitude, $u = u_i + c_s$ is the propagation velocity in the laboratory frame, and D is the spatial width of the soliton. From the theory, there are distinct relationships between the soliton amplitude, width and speed. These relationships are

$$D = \lambda_D \sqrt{6 \frac{n_0}{\delta n}} \quad (2)$$

$$u = u_i + c_s \left(1 + \frac{1}{3} \frac{\delta n}{n_0} \right) \quad (3)$$

where λ_D is the Debye length, u_i is the ion drift speed and $c_s = \sqrt{T_e/m_i}$ is the ion sound speed. From these equations, we see that as the amplitude increases, the width decreases and the velocity increases.

B. Wave packets

In addition to solitons, it has been suggested that plasma wave packets may also be generated in response to the perturbation of the cathode plume mode.¹² The ion acoustic wave packet is a class of plasma oscillation that propagates near the ion acoustic speed that can grow in the presence of a strong electron drift.¹⁶ A common function used to describe these wave packets is the Gaussian wave packet given by

$$g(x, t) = A e^{-\left(\frac{x - ugt}{\ell} \right)^2} e^{i(kx - \omega t)}, \quad (4)$$

where A is the amplitude, u_g is group velocity, and ℓ is the spatial width of the wave packet.¹⁶⁻¹⁸ We will use this Gaussian wave packet definition to determine if the some of the waves we observe in response to the localized perturbation are indeed wave packets.

III. Experimental Configuration

A 20 A class LaB₆ cathode was used to study the instabilities that are generated in plume mode. The cathode has a 1/4" cylindrical LaB₆ insert, a 3 mm tungsten orifice plate, and graphite keeper. This cathode was designed for use in the H6 Hall thruster. The cathode was tested in a diode configuration where the anode was placed 43 mm downstream. The anode was made of a rolled tungsten sheet. An image of the cathode discharging into the anode is shown in Fig. 2. The cathode was operated in a vacuum facility that was 4 ft long and 2 ft in diameter that achieves a base pressure of 0.5 μ Torr-N₂. During this experiment, the cathode was operated at the nominal 20 A of discharge current at a propellant flow rate of 8 sccm. The operating pressure in the vacuum facility was 20 μ Torr-Xe.

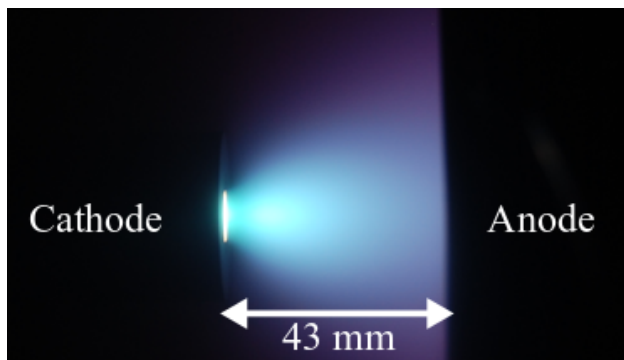


Fig. 2 Cathode discharging into anode.

The properties of the propagating instabilities were measured using a pair of probes that were separated 3 mm. The ion saturation current was collected by biasing these probes to -36 V using four D9 batteries. This current was measured across a 1 k Ω shunt resistor using an oscilloscope. The spatial dependence of the modes was captured by conducting spatial sweeps between the cathode and the anode along the axis of the discharge. Figure 3 shows a schematic of the probe setup.

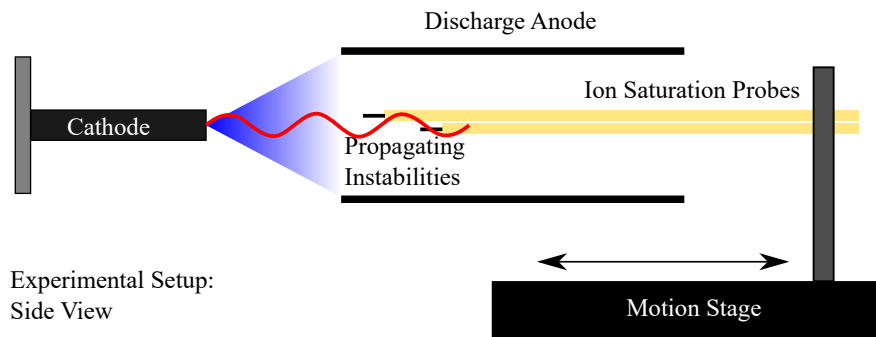


Fig. 3 Side view of the experimental setup. Hollow cathode was operated in a diode configuration and two probes are used to measure wave and plasma properties.

IV. Analysis Techniques

Below, we discuss the analysis techniques used to characterize the waves in the plasma. First we describe the technique used to discriminate between the modes that propagate in the plasma in response to the low frequency perturbation. Second we provide a discussion of the Beall technique for estimating the dispersion and group velocity of the modes in the cathode plume.

Common to the discussion of our analysis techniques is the relationship between the measured ion saturation current and plasma density fluctuations. Assuming quasi-neutrality, we can relate the ion saturation current, I , to the plasma density, n , using cylindrical Langmuir probe theory

$$n = \frac{I}{0.61qA_p} \sqrt{\frac{m_i}{T_e}}, \quad (5)$$

where A_p is the area of the probe, m_i is the ion mass, and T_e is the electron temperature. Assuming that temperature fluctuations are small, we find that

$$\frac{\delta n}{n_0} = \frac{\delta I}{I_0}, \quad (6)$$

where δn is the fluctuation in plasma density, n_0 is the steady state plasma density, δI and I_0 are the fluctuating and steady state ion saturation current, respectively.

A. Decomposition of Modes Using a Continuous Wavelet Transform

The hypothesis explored in this work is that large localized perturbations in the cathode plume disperse energy into the natural modes of the plasma. It is proposed that those modes are composed solitons and wave packets, however there still hasn't been clear detection of constituent waves. To discriminate between these oscillations, we use a continuous wavelet transform and filter the measured signals based on empirical cut-off frequencies. A continuous wavelet transform (CWT) is a mathematical operation that is useful for time-frequency analysis. The CWT uses a wavelet basis function to decompose a signal, in a similar way to a Fourier transform; the CWT also encodes information about duration as well as the amplitude and frequency. The mathematical definition of a wavelet transform is

$$\chi(\omega, \tau) = \sqrt{\omega} \int_{-\infty}^{\infty} x(t) \bar{\psi}(\omega(t - \tau)) dt, \quad (7)$$

where $\chi(\omega, \tau)$ is the amplitude of the wavelet at time τ with frequency ω , $x(t)$ is the input signal (relative density fluctuation) that is transformed, and $\bar{\psi}(t)$ is the wavelet function. Typically wavelets are of the form $\bar{\psi}(t) = w(t)e^{it}$, where $w(t)$ describes the temporal extent of wavelet. We have used a generalized Morse wavelet in our analysis.¹⁹ The output of this analysis, $\chi(\omega, \tau)$, describes how the frequency content of the plasma oscillations is changing in amplitude over time. For example, a purely harmonic oscillation will appear as a single frequency and amplitude that is constant in time. When trying to isolate impulses, such as wave packets or solitons, the Fourier transform can be difficult to use for data filtering because lower frequency components may be important in determining temporal behavior of an oscillation. On the other hand, the CWT can allow you to filter out waves without losing information about the envelope of the oscillations of interest.

B. Beall Technique for Estimation of Dispersion

The Beall technique uses the signal measured by two probes to statistically estimate the dispersion.²⁰ This technique has been used extensively to characterize waves in hollow cathodes.^{11,12,21,22} Here, we provide a qualitative description of the procedure used to estimate the dispersion.

A waveform of 10^6 samples is captured at 10 MHz from each ion saturation probe. This long plasma density waveform is first divided into many sub-waveforms that are individually analyzed. The principle is to compute the Fourier transform of the sub-waveform from both probes and use that information to estimate the phase between the signal as a function of frequency, ω . The wavevector, $k = 2\pi/\lambda$, is then estimated using the phase and probe separation. The signal, however, is buried in noise requiring us to bin and average over many sub-waveforms using the amplitude of the Fourier transform as a weight. After

sufficient averaging, the dispersion of the plasma is elevated above the noise and become apparent. The output of this is a two-dimensional histogram of the cross correlation between frequency and wavevector where the amplitude of each bin is proportional to the energy density of each mode.

There are limits to the kinds of waves that we can observe using this technique. This technique is susceptible to aliasing based on the geometrical properties of the probe array. With our probe spacing of 3 mm, we know that the maximum wavevector (minimum wavelength) is 1047 m^{-1} . Smaller wavelength than this are aliased. In some instances, the dispersion must be anti-aliased by concatenating the dispersion estimates and using physical intuition to interpret the result.

These measurements are used to determine the speed and propagation of the modes in the plasma. The phase and group velocities are calculated by

$$v_{ph} = \frac{\omega}{k} \quad \text{and} \quad v_g = \frac{\partial \omega}{\partial k}. \quad (8)$$

These measurements help us identify the nature of the waves we observe in the cathode plume.

V. Experimental Results & Analysis

Our experiment and analysis techniques were designed to measure the properties of the propagating modes in the plume of the cathode plume. In this section we will discuss our measurements and how they help reinforce the notion that localized perturbation in the plasma consisting of solitons and wave packets propagate away from this source.

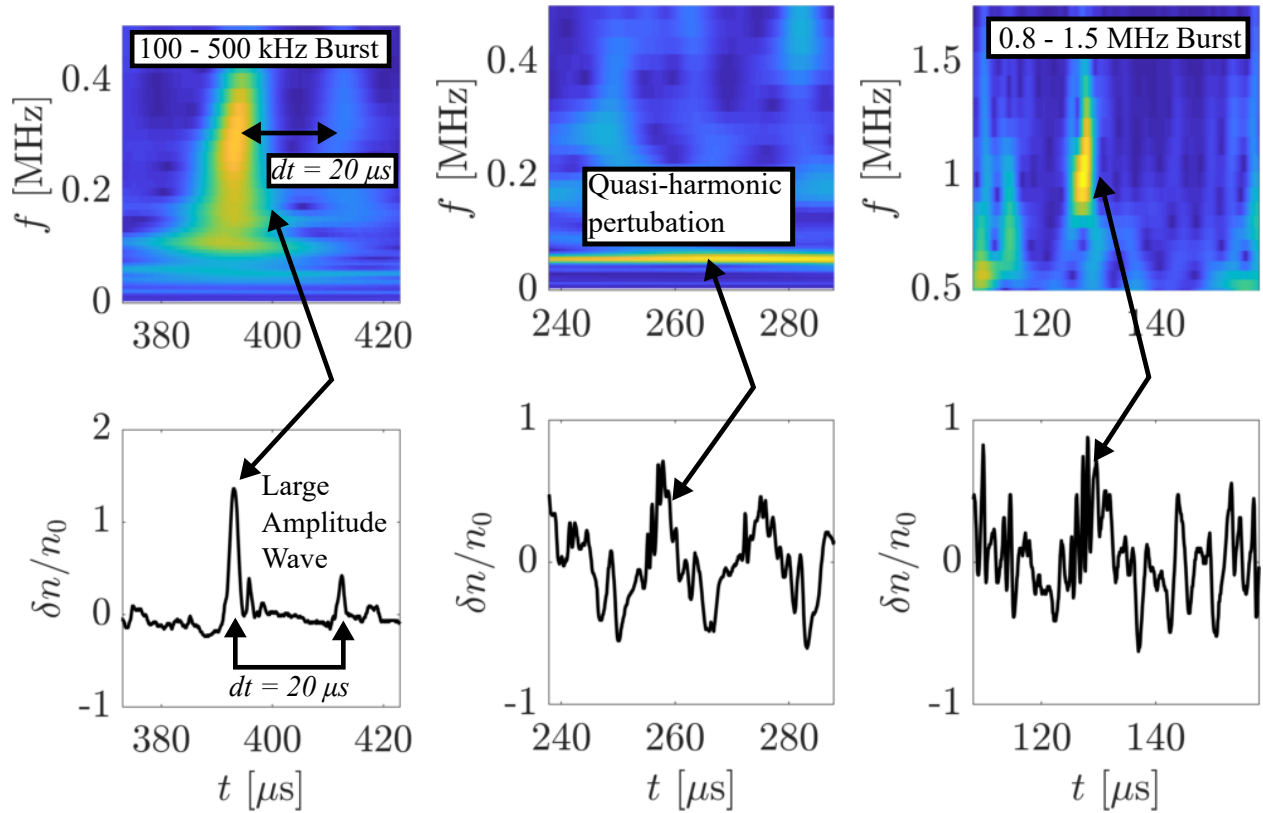
A. Decomposition of Modes

The ion saturation probes are used to measure the plasma density fluctuations. To decompose the different kinds of oscillations, we use a CWT of these traces. Figure 4a to 4c show a section the raw traces (bottom) and their CWT (top) at a few places in the plume of the hollow cathode. Here, the CWT is used to show the amplitude of the frequency components as a function of time. Near the cathode in Fig. 4a, we see that the plume has large amplitude density structures. In the CWT, these waves appear to be associated with bursts of higher frequency content between 0.1 and 0.5 MHz. Furthermore, bursts appear to be separated by about $20 \mu\text{s}$. In other words, these large amplitude waves are generated at a rate of approximately 50 kHz. In the center of the plume, shown in Fig. 4b, we find that these bursts have given way to a quasi-harmonic oscillation in density. This is observed in the CWT as a single frequency of constant amplitude over time. This frequency (period) is approximately 50 kHz ($20 \mu\text{s}$), consistent with the periodicity of the structures observed near the cathode. Lastly, nearer to the anode in Fig. 4c we find that there are bursts of high frequency oscillations in the plasma density and they are associated with modes between 0.8 and 1.5 MHz. Through the examination of Fig. 4, we now have classified the types of waves as being associated with particular frequency bands: 50 kHz, 0.1-0.5 MHz, and 0.8-1.5 MHz. Next we will show the waveforms that are produced by each of these frequency bands and how they combine to create the measured signals.

Using the CWT, we can decompose the signal to establish the contributions from each type of oscillation that was observed in the plasma in Fig. 4. The result of this manipulation is shown in Figs. 5a to 5c. These figures cover the same positions in the plume as in Fig. 4. In Fig. 5a, we find that the 0.1-0.5 MHz oscillations are the primary contributors to the large density structure. Figure 5b shows that the primary mode is the 50 kHz oscillation, however there are still contributions from the 0.1-0.5 MHz waves and the 0.8-1.5 MHz waves. Lastly, Fig. 5c shows that near the anode the 0.8-1.5 MHz waves are the largest component of the plasma density fluctuation.

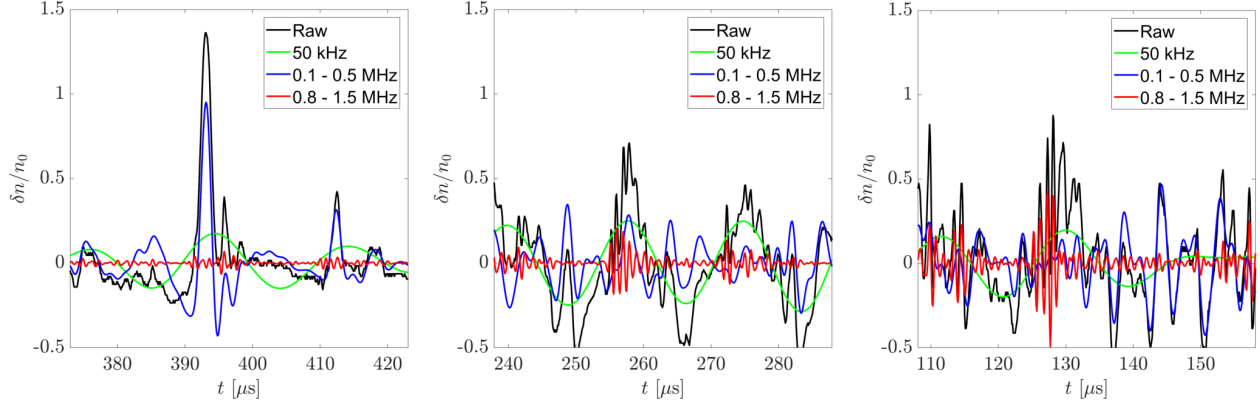
B. Interpretation of Modes

Now that we have been able to decompose the various waves in the plasma, we can further analyze these waveforms to support the interpretation that solitons and wave packets are produced in response to a quasi-periodic perturbation of the cathode plume. The identified frequency bands are interpreted as follows. The 50 kHz band is the quasi-periodic fluctuation of the localized perturbation, the 0.1-0.5 MHz corresponds to the solitons, and 0.8-1.5 MHz are the wave packets. Here, we will analyze and discuss the properties of the source, the solitons, and the wave packets in the context of the theory provided in Section ?? to support this hypothesis.



(a) Position $z = 7$ mm. Near the cathode, large amplitude plasma density fluctuations are correlated with modes between 100 and 500 kHz in the CWT. (b) Position $z = 19$ mm. In the middle of the plume, a quasi-harmonic oscillation of the plasma density is observed. (c) Position $z = 27$ mm. Near the anode, bursts of noise in the density is correlated with 0.8 and 1.5 MHz modes in the CWT.

Fig. 4 Top: Continuous wavelet transform of the ion density fluctuations. The color axis is proportional to wave amplitude. Bottom: Raw ion density fluctuations.



(a) Position $z = 7$ mm. Near the cathode, modes between 0.1 and 0.5 MHz in the CWT are the largest contribution to the density fluctuations.

(b) Position $z = 19$ mm. In the middle of the plume, the 50 kHz is the largest contribution to the density fluctuations, however there are contributions from the other two classifications of waves.

(c) Position $z = 27$ mm. Near the anode, the primary contribution to the density fluctuations comes from the 0.8-1.5 MHz oscillations.

Fig. 5 Contributions to the plasma density fluctuation from the three types of oscillations that have been identified in the cathode plume.

1. Source

Based on high-speed imaging, we know that there is a localized region in the plume from which the instabilities originate. Our claim is that the 50-kHz oscillation is a result of the density oscillation of the source region. We can compare previous estimates of the width of this region from the high-speed camera to the observed wave amplitude profile. To create this profile, we can time average the CWT of the density oscillations and extract the amplitude of the 50-kHz wave and plot it as a function of position. Figure 6 shows the result of this calculation. If we assume that the full-width-half-maximum of the amplitude profile is a good estimator of the width of the source perturbation, we find its width is about 14 ± 2 mm. This is in relatively good agreement with previous observations from high-speed imaging that estimated the width to be on the order of 10 mm.¹¹ Based on this agreement, we conclude that the 50 kHz wave is indeed the oscillation from the localized perturbation in the plume.

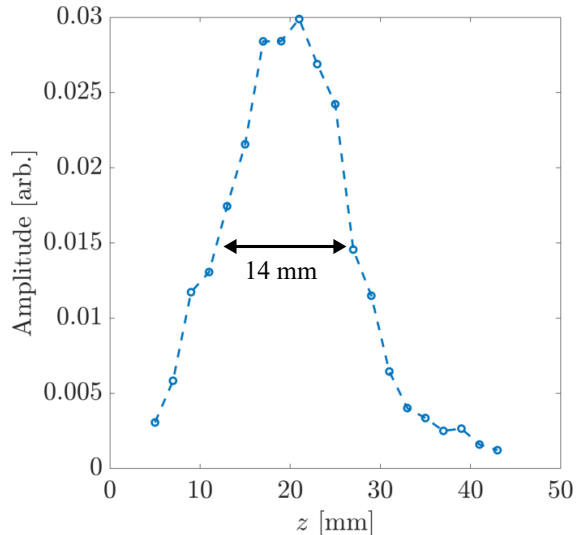


Fig. 6 Source wave amplitude as a function of position. The FWHM is 14 mm.

2. Solitons

A previous experiment has reported the possibility ion-acoustic solitons being generated in the cathode plume in response to the localized perturbation.¹² We note that the waves in the 0.1-0.5 MHz band exhibit similar properties to ion-acoustic solitons, particularly near the cathode. Eqn. 1 was used to curve fit a waveform at $z = 5$ mm. The result of this analysis is shown in Fig. 7. We find that the temporal width is $\tau = 0.598 \mu\text{s}$ and the amplitude is $\delta n/n_0 = 1.044$. Overall, we find good qualitative agreement between the measured waveform and the curve fit. An ion acoustic soliton propagates near the ion acoustic speed. For a

hollow cathode this is typically about 2000 m/s. If we assume the soliton-like structure is propagating with this speed, we find the spatial width to be $D = u\tau \simeq 1$ mm. Furthermore, if we estimate the plasma density (10^{18} - 10^{19} for a typical hollow cathode) we can compare the measured soliton width to the theory. Using these bounds on density we find that the measured waveform is between 30 and 100 times that predicted by analytical theory. This discrepancy is likely due to the simplifying assumptions of the theory. For example, the hollow cathode plume has large density gradients and an ionization on the order of the frequency of these oscillations that could be affect the observed width.

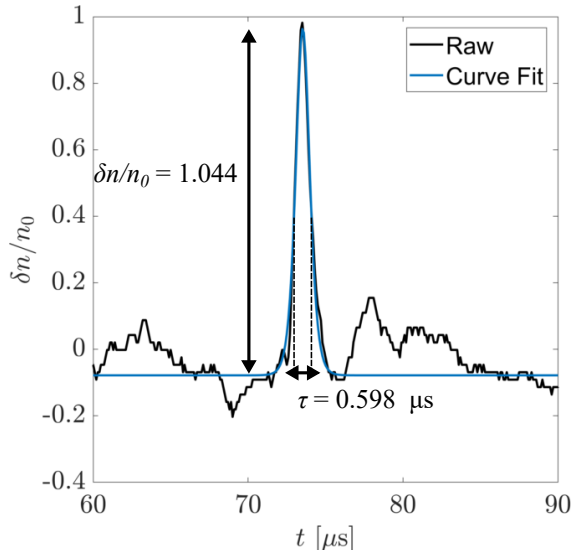


Fig. 7 Curve fit of the raw data using ion-acoustic soliton theory at $z = 5$ mm.

3. Wave packets

Past experiments have suggested that ion acoustic wave packets may be generated in response to the localized perturbation in the cathode plume.¹² In Fig. 5 we find that the wave in the 0.8-1.5 MHz band qualitatively looks like a wave packet. Figure 8a shows a wave packet observed at 43 mm away from the cathode and a curve fit to Eqn. 4. We find that the density profile is in good qualitative agreement with a simple Gaussian wave packet description. The central frequency is found to be 1.3 MHz and the temporal width of the wave packet is estimated to be $1.2 \mu\text{s}$. The ion plasma frequency in the cathode plume is on the order of 100 MHz, therefore these time scales are consistent with ion fluctuations, perhaps indicating that these may be ion-acoustic wave packets.

We can use the Beall dispersion estimation technique to calculate the group velocity of these wave packets. Figure 8b shows the dispersion of the modes in the plasma at 43 mm away from the cathode. We see that in the 0.8-1.5 MHz band, the group velocity of the wave, estimated by a curve fit, is found to be $v_g = 190$ km/s. In relation to the other velocity scales, assuming the electron temperature is about 3 eV,

$$\frac{v_g}{c_s} \simeq 100 \text{ and } \frac{v_g}{v_e} \simeq \frac{1}{4}, \quad (9)$$

where $c_s = \sqrt{qT_e/m_i}$ is the ion sound speed and $v_e = \sqrt{(qT_e/m_e)}$ is the electron thermal speed. The observed velocity of these wave packets is too fast to be consistent with ion-acoustic wave packets. A possible explanation for this is that we have measured the velocity only in the axial direction. It is possible that the waves may be propagating in the radial direction not the axial cause the probes to artificially measure a fast phase velocity.

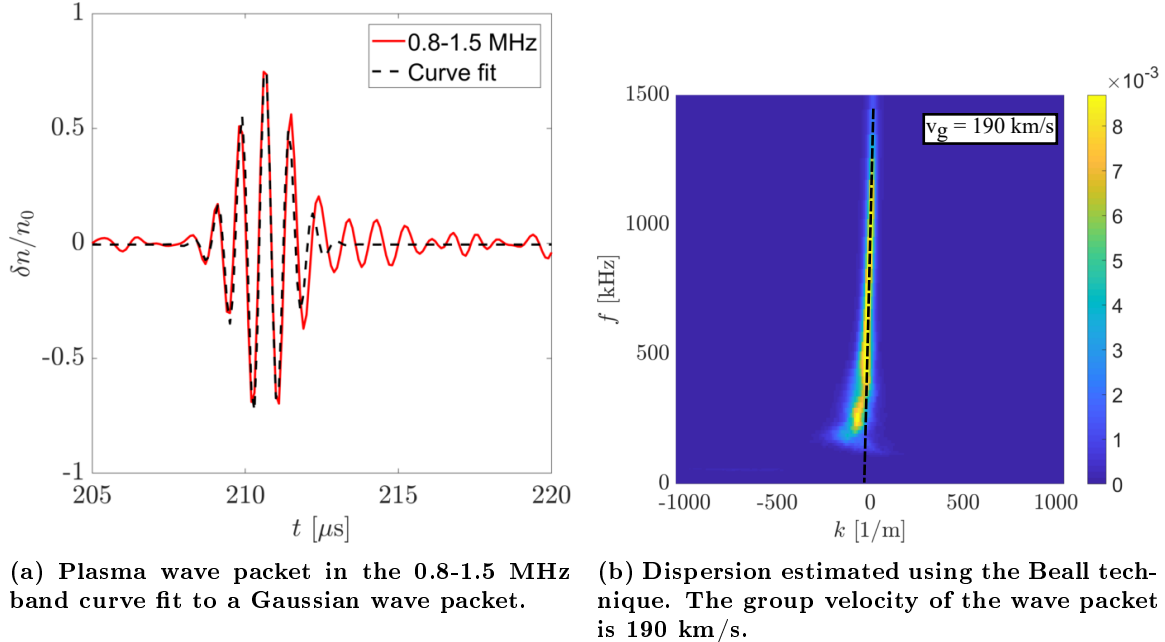


Fig. 8 Analysis of wave packets 43 mm away from the cathode.

VI. Conclusion

The spatial dependence of plasma waves was experimentally characterized using ion saturation probes in the plume of a 20 A hollow cathode while operating in plume mode. The continuous wavelet transform was used to decompose the raw signals into three constituent classes of waves, the source oscillation, solitons, and wave packets. The amplitude of the source oscillation as a function of position was used to determine the width of the perturbation and was shown to be in good agreement with previous estimates from high-speed camera measurements. Furthermore, we have shown that the oscillation in this region of the plume can be decomposed into a combination of wave packets and soliton-like structures. Near the cathode exit, large amplitude density oscillations were measured and interpreted with soliton theory. While we have found good qualitative agreement between our measurements and soliton theory, quantitative estimates of the width determined through curve fitting appear to be 1 to 2 orders of magnitude smaller than our observations. Lastly, we examined wave packet-like oscillations in the cathode plume and shown good qualitative agreement with a Gaussian wave packet, however the measured group velocity of this mode is much too large to be ion acoustic in nature. Together, these experimental results support the hypothesis that a localized perturbation is decomposed into the natural modes of the plasma as solitons and wave packets that propagate away.

Acknowledgments

This work was funded by the NASA Space Technology Research Fellowship grant number NNX15AQ37H.

References

- [1] Sengupta, A., Brophy, J., Anderson, J., Garner, C., Banks, B., and Groh, K., "An Overview of the Results from the 30,000 Hr Life Test of Deep Space 1 Flight Spare Ion Engine," *40th AIAA/ASME/SAE/ASEE Joint Propulsion Conference and Exhibit*, American Institute of Aeronautics and Astronautics, 2004. doi:10.2514/6.2004-3608.
- [2] Csiky, G. A., "Measurements of Some Properties of a Discharge from a Hollow Cathode," *NASA Technical Note*, 1969.
- [3] Mikellides, I. G., Katz, I., Goebel, D. M., Jameson, K. K., and Polk, J. E., "Wear Mechanisms in Electron

- Sources for Ion Propulsion, II: Discharge Hollow Cathode,” *Journal of Propulsion and Power*, Vol. 24, No. 4, 2008, pp. 866–879.
- [4] Sary, G., Garrigues, L., and Boeuf, J.-P., “Hollow Cathode Modeling: I. A Coupled Plasma Thermal Two-Dimensional Model,” *Plasma Sources Science and Technology*, Vol. 26, No. 5, 2017, p. 055007. doi:10.1088/1361-6595/aa6217.
 - [5] Sary, G., Garrigues, L., and Boeuf, J.-P., “Hollow Cathode Modeling: II. Physical Analysis and Parametric Study,” *Plasma Sources Science and Technology*, Vol. 26, No. 5, 2017, p. 055008. doi:10.1088/1361-6595/aa6210.
 - [6] Philip, C., “A Study of Hollow Cathode Discharge Characteristics,” *AIAA Journal*, Vol. 9, No. 11, 1971, pp. 2191–2196. doi:10.2514/3.50024.
 - [7] Kerslake, W. R., and Rawlin, V. K., “SERT II - Durability of the Hollow Cathode and Future Applications of Hollow Cathodes,” *Journal of Spacecraft and Rockets*, Vol. 7, No. 1, 1970, pp. 14–20. doi:10.2514/3.29856.
 - [8] Fife, J., Martinez-Sanchez, M., and Szabo, J., “A Numerical Study of Low-Frequency Discharge Oscillations in Hall Thrusters,” American Institute of Aeronautics and Astronautics, 1997. doi:10.2514/6.1997-3052.
 - [9] Goebel, D. M., Wirz, R. E., and Katz, I., “Analytical Ion Thruster Discharge Performance Model,” *Journal of Propulsion and Power*, Vol. 23, No. 5, 2007, pp. 1055–1067. doi:10.2514/1.26404.
 - [10] Mandell, M., and Katz, I., “Theory of Hollow Operation in Spot and Plume Modes,” American Institute of Aeronautics and Astronautics, 1994. doi:10.2514/6.1994-3134.
 - [11] Georgin, M. P., Jorns, B. A., and Gallimore, A. D., “An Experimental and Theoretical Study of Hollow Cathode Plume Mode Oscillations,” Electric Rocket Propulsion Society, Atlanta Georgia, 2017.
 - [12] Georgin, M. P., Jorns, B. A., and Gallimore, A. D., “Experimental Evidence for Ion Acoustic Solitons in the Plume of a Hollow Cathode,” Sevilla, Spain, 2018, p. 12.
 - [13] Washimi, H., and Taniuti, T., “Propagation of Ion-Acoustic Solitary Waves of Small Amplitude,” *Physical Review Letters*, Vol. 17, No. 19, 1966, pp. 996–998. doi:10.1103/PhysRevLett.17.996.
 - [14] Ikezi, H., Taylor, R. J., and Baker, D. R., “Formation and Interaction of Ion-Acoustic Solitons,” *Physical Review Letters*, Vol. 25, No. 1, 1970, pp. 11–14. doi:10.1103/PhysRevLett.25.11.
 - [15] Watanabe, S., “Formation and Recurrence of Ion Wave Solitons,” *Journal of Plasma Physics*, Vol. 13, No. 2, 1975, pp. 217–230. doi:10.1017/S0022377800026003.
 - [16] Hamza, A. M., “On the Development and Evolution of Nonlinear Ion Acoustic Wave Packets,” *Ann. Geophys.*, Vol. 23, No. 6, 2005, pp. 2249–2257. doi:10.5194/angeo-23-2249-2005.
 - [17] Denavit, J., and Sudan, R. N., “Effect of Trapped Particles on the Nonlinear Evolution of a Wave Packet,” *Physical Review Letters*, Vol. 28, No. 7, 1972, pp. 404–407. doi:10.1103/PhysRevLett.28.404.
 - [18] Goldman, M. V., “Strong Turbulence of Plasma Waves,” *Reviews of Modern Physics*, Vol. 56, No. 4, 1984, pp. 709–735. doi:10.1103/RevModPhys.56.709.
 - [19] Olhede, S. C., and Walden, A. T., “Generalized Morse Wavelets,” *IEEE Transactions on Signal Processing*, Vol. 50, No. 11, 2002, pp. 2661–2670. doi:10.1109/TSP.2002.804066.
 - [20] Beall, J. M., Kim, Y. C., and Powers, E. J., “Estimation of Wavenumber and Frequency Spectra Using Fixed Probe Pairs,” *Journal of Applied Physics*, Vol. 53, No. 6, 1982, pp. 3933–3940. doi:10.1063/1.331279.
 - [21] Jorns, B. A., Mikellides, I. G., and Goebel, D. M., “Investigation of Energetic Ions in a 100-A Hollow Cathode,” *50th AIAA/ASME/SAE/ASEE Joint Propulsion Conference*, 2014, p. 3826.
 - [22] Jorns, B., Lopez Ortega, A., and Mikellides, I. G., “First-Principles Modelling of the IAT-Driven Anomalous Resistivity in Hollow Cathode Discharges I: Theory,” American Institute of Aeronautics and Astronautics, 2016. doi:10.2514/6.2016-4626.